PCCP

Accepted Manuscript

ROYAL SOCIETY OF CHEMISTRY

www.rsc.org/pccp

ARTICLE TYPE
www. rsc.org/xxxxxx | XXXXXXXX

Size effects induced high thermoelectric figure of merit in PbSe and PbTe nanowires

Ernesto O. Wrasse,[a] **Alberto Torres,**[b‡] **Rogério J. Baierle,**[c] **Adalberto Fazzio,**[b‡] **and Tome M. Schmidt,**[* a]

The fundamental properties that compose the thermoelectric figure of merit are investigated in confined systems PbSe and PbTe nanowires, with the goal to improve the thermoelectric efficiency. Using the Landauer electronic transport theory, we verify that the figure of merit can be several times larger than the bulk value for nanowires with diameters down to one nanometer scale. This enhancement in the thermoelectric efficiency is primary due to the reduction of the thermal conductivity, and an increasing in the power factor. The origin of these desired properties that enable to transform heat into electricity comes from the confinement effects, which increase the density of states around the Fermi level, either for *n*- or *p*-type system.

1 Introduction

The increasing demand for energy, results in the searching for new energy sources, especially clean and renewable ones. In this way thermoelectric devices are good candidates, because they can transform solar energy and heat into electricity.[1] Thermoelectric power generations are based in the Seebeck effect, in which a temperature gradient is directly converted in electric current. The limitation of these devices is the efficiency, that is very low when compared to devices which utilize other energy sources. In this way, the searching for materials is essential to increase the thermoelectric power efficiency.

The adimensional figure of merit ZT is used to quantify the efficiency of a thermoelectric device. It is writing as:

$$ZT = \frac{GS^2}{\kappa_{el} + \kappa_{ph}} T, \qquad (1)$$

where G is the electric conductance, S is the Seebeck coefficient, κ_{el} and κ_{ph} are the electron and phonon contributions to the total thermal conductivity, respectively, and T is the absolute temperature of the device. In the 1950's decade a great number of works were dedicated to obtain efficient thermoelectric materials, but the largest ZT obtained was smaller than 1,[2] an efficiency too low to be used in thermoelectric devices.

The low efficiency observed in bulk materials reduced the interest of thermoelectric properties, and for many years the study of these properties was latent. A new light in this matter was given by Lin and Dresselhaus, using nanostructured systems.[3,4] They developed a theoretical model to describe the thermoelectric properties, predicting that nanostructures can have greater thermoelectric efficiency than the bulk ones. With this new proposals the interest of thermoelectric properties in nanostructured systems has increased.[5–9] Bulk PbSe and PbTe are already promising thermoelectric materials. They crystallize in the rock salt structure and are narrow band gap semiconductors. They have one of the largest value of ZT for bulk materials, making nanostructures of PbSe and PbTe natural candidates to increase even more the thermoelectric efficiency. A special type of nanostructure of PbSe and PbTe are nanowires (NW), that already have been synthesized.[10–13] Alloys and nanostructures of lead chalcogenides have been showed to increase the efficiency, reaching a ZT up to 2.[14–16] Another efficient strategy to enhance the ZT of lead chalcogenides is the doping with impurities that introduces resonant levels near the valence band maximum or conduction band minimum.[17–20]

In this work we investigate the fundamental properties involved to obtain ZT, which are the electric conductance, Seebeck coefficient and thermal conductivity for several nanowire diameters. The results reveal that the increasing of the thermoelectric efficiency by reducing the nanowire diameter is due to two main factors: the reduction of the thermal conductivity, and an increasing of the power factor ($PF = GS^2$). We will show that the enhancement of ZT is due to the distortion in the density of states around the Fermi level, as a result of the electronic confinement effect.

2 Methodology

The thermoelectric properties of PbSe and PbTe NWs are investigated employing the Landauer-Büttiker approach,[21,22] where the quantities involved in the equation for ZT are obtained separately. In this model the electric conductance, Seebeck coefficient and electronic thermal conductivity can be writing in terms of the electronic transmittance $T(\varepsilon)$, in the following way:

---

[a] *Instituto de Física, Universidade Federal de Uberlândia, Uberlândia, MG, Brazil. Tel: 55 34 3239 4190; E-mail: tschmidt@infis.ufu.br*
[b] *Instituto de Física, Universidade de São Paulo, São Paulo, SP, Brazil.*
[c] *Departamento de Física, Universidade Federal de Santa Maria, Santa Maria, RS, Brazil.*

$$G = \chi^{(0)}, \tag{2}$$

$$S = -\frac{1}{eT}\frac{\chi^{(1)}}{\chi^{(0)}}, \tag{3}$$

$$\kappa_{el} = \frac{1}{e^2 T}\left[\chi^{(2)} - \frac{(\chi^{(1)})^2}{\chi^{(0)}}\right], \tag{4}$$

where e is the electron charge, and T is the operation temperature. The χ_s' are defined as:

$$\chi^{(\alpha)} = \int d\varepsilon \left(-\frac{\partial f}{\partial \varepsilon}\right)(\varepsilon - \mu)^{\alpha} T(\varepsilon). \tag{5}$$

Here f is the electronic Fermi distribution, μ is the electronic potential, and $T(\varepsilon)$ is the electronic transmittance. By neglecting the phonon contribution to the total κ ($\kappa_{ph} = 0$), the figure of merit ZT can be written in terms of the χ_s' as:

$$ZT = \left[\frac{\chi^{(0)}\chi^{(2)}}{[\chi^{(1)}]^2} - 1\right]^{-1}. \tag{6}$$

For 1D systems, $T(\varepsilon)$ is given by the number of energy bands at energy ε, that is equal to the number of transport channels available. Thus we obtain $T(\varepsilon)$ from an electronic structure calculation, so that in this approximation we do not differentiate the electrodes from the scattering region.

The electronic properties are obtained within the density functional theory, where the exchange-correlation term is described by the general gradient approximation.[23] The interaction between core and valence electrons is described by the projected augmented wave method.[24] Fully relativistic calculations are performed by including the spin-orbit interaction as implemented in the Vienna Ab Initio Simulation Package.[25,26] The Kohn-Sham orbitals are expanded in a basis set of plane waves, with an energy cutoff of 450 eV. We use periodic boundary conditions along the NW growth direction, and to avoid undesirable interactions between the NW images a vacuum size of $1nm$ between them have been used. The Brillouin zone was sampled by a center scheme, by using a number of k points up to $1 \times 1 \times 4$ Monkhorst-Pack form,[27] such that the total energy was converged.

3 Results and Discussions

We study the thermoelectric properties of PbSe and PbTe NWs with diameters between 1 and 4 nm, where the confinement effects are very strong. These NWs are classified according to the in-plane stoichiometry, so that NWs that have a 1 : 1 in-plane stoichiometry are called type I NWs and those that do not keep the 1 : 1 in-plane stoichiometry are called type II NWs, as showed in Fig. 1. The electronic properties of PbSe and PbTe NWs are different for type I and type II, which are affected by three effects: quantum confinement, spin-orbit interaction, and in-plane stoichiometry, as shown before.[28]

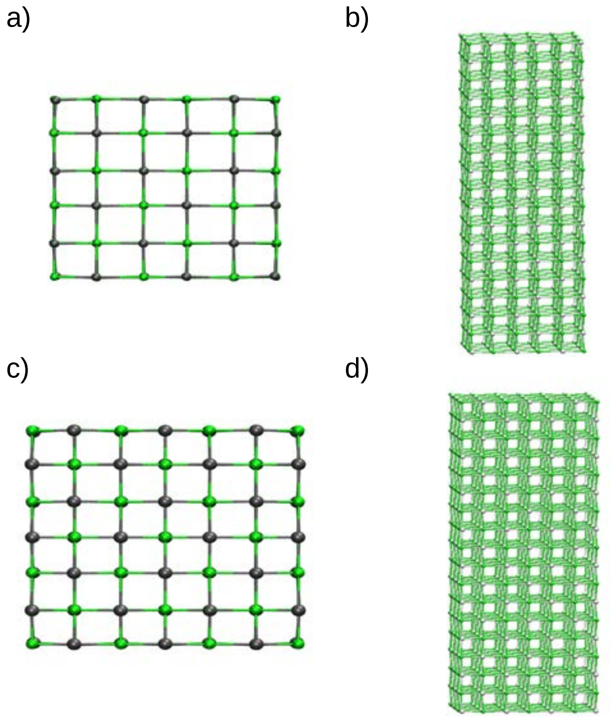

Fig. 1 Top and side view of PbSe NWs aligned along the (001) direction. In (a) and (b) are the atomic geometry for a type I NW, and in (c) and (d) for a type II NW. The small (green) spheres represent the Se atoms and the bigger (white) spheres represent the Pb atoms.

The thermoelectric properties of type I and type II NWs are analyzed separately. As we can see in Fig.2, for type I PbSe NWs the Seebeck coefficient S increases when the system is confined, but this effect is compensated by a decreasing of the conductance G. The ZT increases by decreasing the NW diameter, mainly due to the reduction of the thermal conductivity κ_{el}. This reduction is so substantial that the difference of κ_{el} between the thinner and the thicker NW is four orders of magnitude, leading to a huge ZT for very thin NW diameter. In this picture we do not consider the κ_{ph} contribution to the total κ. It is known that the reduction of κ_{ph} is dominant for the enhancement of ZT for semiconductor nanostructures.[29–31] So, by neglecting κ_{ph} we will be in an ideal situation where phonon transport is completely suppressed. In this way, Fig. 2 can be interpreted as the upper limit for the ZT.

For type II PbSe NWs the dependence of the thermoelectric properties with the diameter is similar to the ones observed in type I, as can be seen in Fig. 3. However, the variables involved in the equation for ZT are quite different in type II as compared to type I. For type II S is lower than that of type

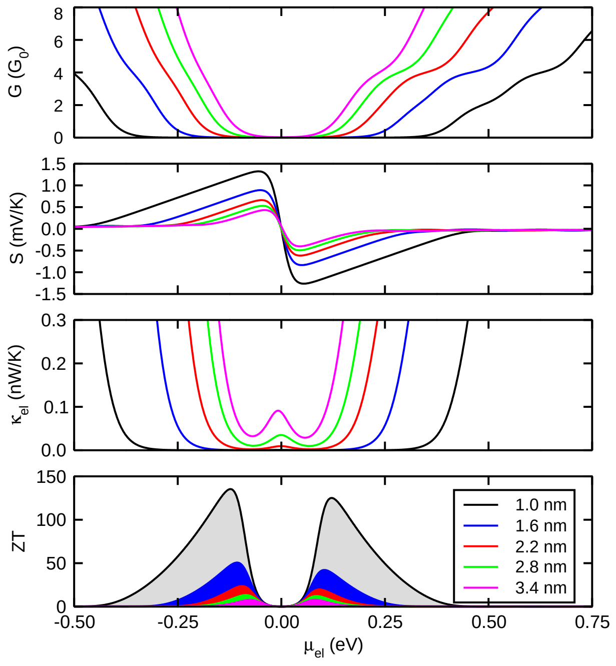

Fig. 2 Thermoelectric properties of type I PbSe NWs as a function of the electronic chemical potential μ_{el}, calculated at $300K$. From top to bottom, the conductance G, the Seebeck coefficient S, the electronic thermal conductivity κ_{el}, and the adimensional figure of merit ZT. The Fermi energy is inside the band gap at zero energy of μ_{el}.

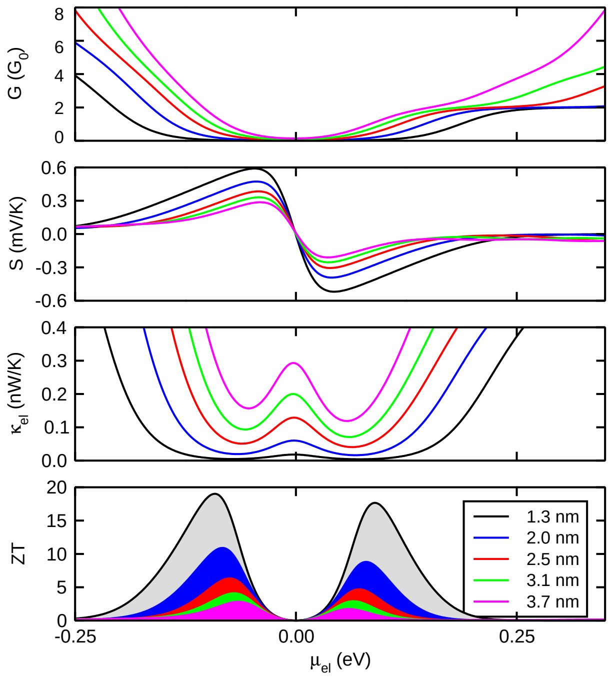

Fig. 3 Thermoelectric properties of type II PbSe NWs as a function of the electronic chemical potential μ_{el}, calculated at $300K$. From top to bottom, the conductance G, the Seebeck coefficient S, the electronic thermal conductivity κ_{el}, and the adimensional figure of merit ZT. The Fermi energy is inside the band gap at zero energy of μ_{el}.

I, but the conductance is so high in type II that compensates the reduction in S. As a result the power factor of type II PbSe NWs is larger than that of type I, as can be seen in Fig. 4. But there is another limiter for the ZT, the thermal conductivity for type II, although it is reduced for small diameter, κ_{el} is one order of magnitude larger than that of type I. As a consequence the thermoelectric efficiency is reduced, so that the ZT in type II PbSe NWs are lower than that of type I, but is still quite high as compared to the experimental bulk value, 0.35.

By looking at the peaks of ZT in Fig. 2 and 3 it is clear that the values of ZT are very high either for the Fermi level located at the valence band (p-type) as well at the conduction band (n-type). Also we observe that both types of NWs present high ZT, however the ZT peaks for type I PbSe NWs (Fig. 2) are almost one order of magnitude larger than that of type II PbSe NWs (Fig. 3). These values must be interpreted as maximum values for ZT, because we do not include the contribution of phonons to κ, although it is know that the reduction of the κ_{ph} is more important than that of κ_{el}.[29–31] Experimental results show that in the bulk phase the major contribution to the total thermal conductivity comes from the phonons, which are 91.6% for PbSe, and 90.3% for PbTe.[32] We will not include κ_{ph} here, but by assuming the bulk ratio $\kappa_{el}/\kappa = 0.084$ for PbSe, we compute the figure of merit as a function of the NW diameter, shown in Fig. 4. As the reduction of κ_{ph} in confined systems is larger than the reduction of κ_{el}, these values can be interpreted as the lower limit for the ZT. The ZT for the thinner type I PbSe NW is 11.4 and for type II PbSe NW the optimized ZT is 0.7. So, we have now the upper limit for the ZT, when no phonon scattering is presented, and the lower limit, when the phonon contribution is the same as the bulk one, both showed in Fig. 4. In this way the ZT will be always inside the hachured range showed in Fig. 4, and even for the lower limit the ZT values are quite high, larger than that of the bulk PbSe, 0.35.

In order to understand why the quantum confinements in PbSe and PbTe NWs give an exceptional enhancement in the thermoelectric efficiency as compared to the bulk, we also plotted in Fig. 4 the power factor PF as well as the electronic thermal conductivity. For very thin NW the small thermal conductivity is responsible for the huge ZT, since the PF is also small. For thicker NW the PF increases but the thermal conductivity also increases. The competition between these two variables result in a total reduction of the ZT by increasing the NW diameter. Also from this picture we can understand why type I and type II present different thermoelectric efficiencies.

Type II has larger thermal conductivity, and the *PF* does not follow the same trend as that of type I, resulting in a smaller *ZT*.

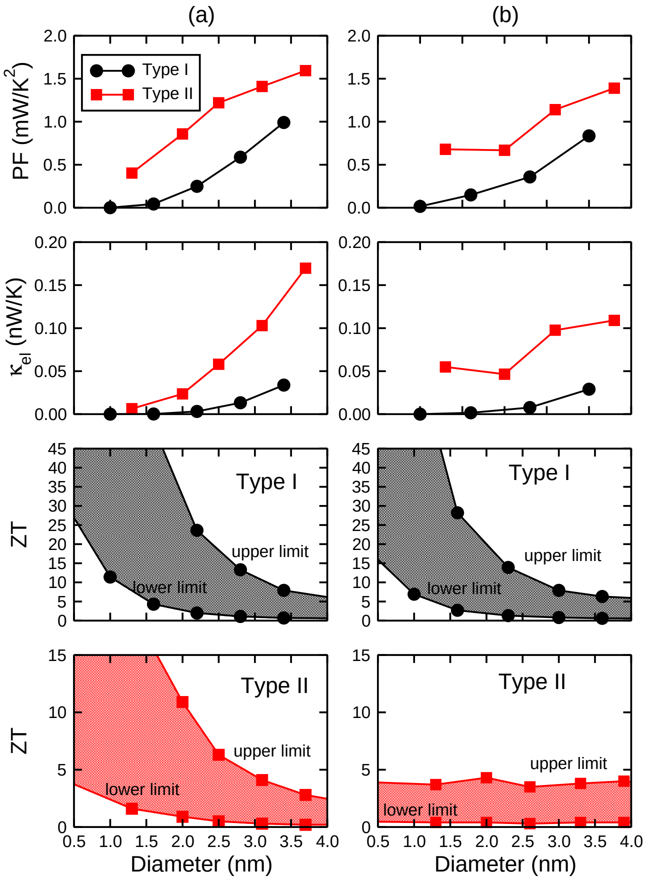

Fig. 4 Calculated power factor, electronic thermal conductivity, and optimized figure of merit as a function of NW diameter for PbSe (a) and PbTe (b). Black spheres represent type I NWs, and red squares type II NWs. The lines are guide for the eyes. All results are obtained at 300K.

The thermoelectric properties of PbTe NWs are not the same as that of PbSe NWs. Although there is an increasing of the *ZT*, especially for type I PbTe NWs, as a result of the nano effects, the gain for thermoelectric applications using PbTe is smaller than that of PbSe nanostructure. This reduction is related to the smaller electronic quantum confinement observed in PbTe NWs as compared to the PbSe. As showed before[28] the spin-orbit effect is size dependent, resulting in a small dependence of the band gap with the NW diameter for PbTe NWs. Small confinement effect means less changes on the density of states. As a consequence, the *ZT* is less affected, as can be seen especially for type II PbTe NWs, Fig. 4-b. By assuming the bulk ratio $\kappa_{el}/\kappa = 0.097$, the lower limit for *ZT* is 6.9 and 0.6 for the thinner and thicker type I PbTe NW, respectively. The upper limit of *ZT* for type I PbTe NW is quite high. On the other hand, for type II PbTe NWs, while the lower limit is small, the upper limit for *ZT* is around 4 for all NW diameters. Also by comparing PbTe with PbSe, for very thin NWs we observe a reduction of the PbTe *ZT* by a factor of 2 as compared to the same diameter of PbSe NWs. For thicker NWs the values of *ZT* are almost the same for both materials.

The origin of the *ZT* enhancement due to the quantum confinement can be better understood by looking the density of states (DOS) around the gap region. The DOS is related to the Seebeck coefficient as well the electronic thermal conductivity. An increasing in the DOS peak is expected an enhancement in *ZT*.[33] From equations (2) to (5) we observe that an increasing in the DOS peak will result in an increasing of the transmittance. This effect will provoke an increasing of the Seebeck coefficient and a decreasing of the κ_{el}. In Fig. 5 the DOS of PbSe NW is plotted for several NW diameters. The DOS peak at left corresponds to valence band maximum, while the first peak for positive values of energy is the conduction band minimum. We clearly can see an increasing of the DOS around the Fermi level, by decreasing the NW diameter. For NW diameter around one nanometer scale the DOS peak is quite high, resulting in a huge *ZT*. As the optimized values for the *ZT* are proportional to the DOS peak plotted in Fig. 5, we also conclude that the electronic structure is the major factor to define the thermoelectric efficiency in confined systems. The reduction of the *PF* with the diameter, showed in Fig. 4 is due to a reduction of the conductance. The competition between *S* and *G* result in a smooth decreasing of the *PF*. On the other hand there is a drastic reduction on the κ_{el} leading to a high value of *ZT*, for thin NW diameters. Based on the results presented here, for thicker NWs with diameter larger than 4 nm, we expect a continuous reduction of the *ZT*, since all variables (as showed in Fig. 4) present a smooth behavior as a function of the NW diameter. Defects and scattering due to surface effects is important to determine the thermoelectric efficiency, especially for thin NWs,[30] but here we have NWs with clean surfaces, and the main factor on the thermoelectric properties is the size effect.

4 Conclusions

In summary, based on transport properties obtained from *ab initio* calculations, we demonstrate that NWs of lead chalcogenides present desired properties to be used as efficient thermoelectric materials. We verify that the figure of merit of PbSe NWs can be several times larger than the bulk one for NW diameter down to one nanometer scale. The main reason for the huge *ZT* for very thin NW diameter is the reduction of the thermal conductivity. For thicker NWs the power factor increases, resulting also in a high *ZT*. This enhancement of the

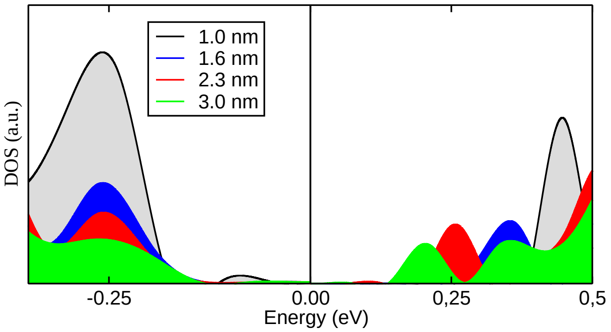

Fig. 5 Density of states around the gap region of type I PbSe NWs for several NW diameters. The solid vertical line is the Fermi level.

ZT is due to an increasing of the density of states, as a consequence of the electronic confinement, which acts different for the bands above and bellow the Fermi level, resulting in a high *ZT* for both *n*- or *p*-type doping. Our results demonstrate that size effects are crucial in the search for potential thermoelectric materials. In this search, we show that PbSe and PbTe NWs present ideal properties to transform heat into electricity.

Acknowledgements

We thank the financial support of the Brazilian agencies CNPq, CAPES, FAPEMIG and computational facilities of Cenapad.

References

1 G. Chen, M. S. Dresselhaus, G. Dresselhaus, J. P. Fleurial and T. Caillat, Int. Mater. Rev. **48**, 45 (2003).
2 F.D. Rosi, Solid-State Electron. **11**, 833 (1968).
3 L.D. Hicks, and M.S. Dresselhaus, Phys. Rev. B **47**, 12727 (1993).
4 L.D. Hicks, and M.S. Dresselhaus, Phys. Rev. B **47**, 16631 (1993).
5 C. J. Vineis, A. Shakouri, A. Majumdar, and M. G. Kanatzidis, Adv. Mater. **22**, 3970 (2010).
6 Y.M. Lin, X.Z. Sun, and M.S. Dresselhaus, Phys. Rev. B **62**, 4610 (2000).
7 T. Markussen, A.-P. Jauho, and M. Brandbyge, Phys. Rev. B **79**, 035415 (2009).
8 J. Zhou, C. Jin, J.H. Seol, X. Li, and L. Shi, Appl. Phys. Lett. **87**, 133109 (2005).
9 Q. Yao, L. Chen, W. Zhang, S. Liufu, and X. Chen, ACS Nano **4**, 2445 (2010).
10 M. Fardy, A.I. Hochbaum, J. Goldberger, M.M. Zhang, and P. Yang, Adv. Mat. **19**, 3047 (2007).
11 W. Liang, A.I. Hochbaum, M. Fardy, O. Rabin, M. Zhang, and P. Yang, Nano Lett. **9**, 1689 (2009).
12 G. Tai, B. Zhou, and W.L. Guo, J. Phys. Chem. C **112**, 11314 (2008).
13 J.W. Roh, S.Y. Jang, J. Kang, S. Lee, J.-S. Noh, W. Kim, J. Park, and W. Lee, Appl. Phys. Lett. **96**, 103101 (2010).
14 K. Biswas, J. Q. He, Q. C. Zhang, G. Y. Wang, C. Uher, V. P. Dravid and M. G. Kanatzidis, Nat. Chem. **3**, 160 (2011).
15 J. Androulakis, C. H. Lin, H. J. Kong, C. Uher, C. I. Wu, T. Hogan, B. A. Cook, T. Caillat, K. M. Paraskevopoulos and M. G. Kanatzidis, J. Am. Chem. Soc. **129**, 9780 (2007).
16 K. F. Hsu, S. Loo, F. Guo, W. Chen, J. S. Dyck, C. Uher, T. Hogan, E. K. Polychroniadis and M. G. Kanatzidis, Science **303**, 818 (2004).
17 Q. Zhang, H. Wang, W. Liu, H. Wang, B. Yu, Q. Zhang, Z. Tian, G. Ni, S. Lee, K. Esfarjani, G. Chen, and Z. Ren, Energ. Environ. Sci. **5**, 5246 (2012).
18 Q. Zhang, F. Cao, K. Lukas, W. Liu, K. Esfarjani, C. Opeil, D. Broido, D. Parker, D.J. Singh, G. Chen, and Z. Ren, J. Am. Chem. Soc. **134**, 17731 (2012).
19 J.P. Heremans, B. Wiendlocha, and A.M. Chamoire, Energ. Environ. Sci. **5**, 5510 (2012).
20 Y. Pei, A. LaLonde, S. Iwanaga, and G.J. Snyder, Energ. Environ. Sci. **4**, 2085 (2011).
21 M. Büttiker, I. Imry, R. Landauer, and S. Pinhas, Phys. Rev. B **31**, 6207 (1985).
22 M. Büttiker, Phys. Rev. Lett. **57**, 1761 (1986).
23 J.P. Perdew, K. Burke, and M. Ernzerhof, Phys. Rev. Lett **77**, 3865 (1996).
24 P.E. Blöchl, Phys. Rev. B **50**, 17953 (1994).
25 G. Kresse and J. Furthmuller, Phys. Rev. B **54**, 11169 (1996).
26 G. Kresse and J. Furthmuller, Comput. Mater. Sci. **6**, 15 (1996).
27 H.J. Monkhorst and J.D. Pack, Phys. Rev. B **13**, 5188 (1978).
28 E.O. Wrasse, R.J. Baierle, T.M. Schmidt, and A. Fazzio, Phys. Rev. B **84**, 245324 (2011).
29 J.W. Roh, S.Y. Jang, J. Kang, S. Lee, J.-S. Noh, W. Kim, J. Park, and W. Lee, APL **96**, 103101 (2010).
30 C.C. Yang, J. Armellin and S. Li, J. Phys. Chem. B **112**, 1482 (2008).
31 C.C. Yang and S. Li, Chem. Phys. Chem. **12**, 3614 (2011).
32 Y.-L. Pei, and Y. Liu, J. Alloys Comp. **514**, 40 (2012).
33 J. P. Heremans, V. Jovovic, E. S. Toberer, A. Saramat, K. Kurosaki, A. Charoenphakdee, S. Yamanaka, and G. J. Snyder, Science **321**, 554 (2008).